MR Appearance of Rhinoscleroma

Ahmed Abdel Khalek Abdel Razek and Ahmed Ahmed Elasfour

BACKGROUND AND PURPOSE: **We describe the MR imaging appearance of rhinoscleroma, an endemic, chronic, granulomatous disease whose causative agent is *Klebsiella rhinoscleromatis*.**

METHODS: **The study included 15 patients (nine males and six females; mean age, 25 years; range, 13–36 years) with rhinoscleroma. MR imaging was performed in all patients. The signal intensity of the nasal masses was compared with that of fat, muscle, and CSF on both T1- and T2-weighted images. All cases were proved by histopathologic examination.**

RESULTS: **The nasal masses were bilateral and symmetrical (n = 6), asymmetrical (n = 4), or unilateral (n = 5). They extended through the anterior nares (n = 9) or posterior choana into the nasopharynx (n = 3). They obstructed the ostiomeatal units with retained secretions in the related sinuses (n = 10). On T1-weighted images, rhinoscleroma showed striking (n = 9) or mild (n = 6) high signal intensity relative to muscle and CSF, but less hyperintensity than fat. On T2-weighted images, the nasal masses showed homogeneous high signal intensity (n = 10) or heterogeneous high signal intensity associated with hypointense foci (n = 5). They were hyperintense relative to fat and muscle, but less hyperintense than CSF.**

CONCLUSION: **The hypertrophic stage of rhinoscleroma has characteristic mild to marked high signal intensity on both T1- and T2-weighted MR images.**

Rhinoscleroma is an endemic, chronic, slowly progressive granulomatous disease caused by *Klebsiella rhinoscleromatis*. The rate of occurrence is probably associated with poverty, poor hygiene, and prolonged contact with infected individuals. There is a familial predisposition, probably owing to infection by intimate contact. Rhinoscleroma is endemic in some parts of Africa, Asia, eastern Europe, South America, and Central America. The disease most frequently affects persons in the 20- to 40-year age range. The nose is the most common site of infection, although the nasopharynx, paranasal sinuses, and pharynx may be involved as well (1–4).

The disease develops in three stages: 1) The rhinitic stage with thickened mucosa, in which histologic study reveals squamous metaplasia and granulation tissue. 2) The hypertrophic stage, characterized by masses of granulation tissue without ulceration; on histologic examination, these masses are formed of plasma cells, Russell bodies (reddish violet elliptical structures, slightly bigger than plasma cells and thought to represent degenerated plas-

ma cells), and Mikulicz cells (foamy histocytes containing *K. rhinoscleromatis*). 3) The final stage of rhinoscleroma has the gross and histologic appearance of scar tissue; isolated foci of plasma cells and Mikulicz cells may be present (4, 5).

Electron microscopic studies have shown the transformation of plasma cells into Russell bodies (6). Further ultrastructural work has demonstrated the different stages of distension of the rough endoplasmic reticulum up to the formation of Russell bodies inside the reactive plasma cells, thus supporting the theory of an intracellular formation of Russell bodies (7). Histochemical studies have indicated a high content of mucopolysaccharides around the walls of the *Klebsiella* organism, suggesting that this may be responsible for protecting the organism against antibiotic therapy (8).

Clinical presentation may be classified into three stages: 1) The catarrhal, granulomatous, and sclerotic stage, in which the rhinitic (catarrhal) stage is seen early. The patient has symptoms similar to those of the common cold, including headache, variable dyspnea, and fetid odor. This stage lasts for several months, during which diagnosis is seldom made. 2) The hypertrophic (granulomatous) stage is characterized by extensive granuloma formation. The tissue at the tip of the nose becomes infiltrated, hard, and nodular. The nose broadens and becomes firmly fixed to the face. The tissue becomes more thickened until breathing is more or less occluded. This stage can evolve over months

FIG 1. Bilateral symmetrical rhino-scleroma.

A, Sagittal T1-weighted image (600/20) shows a large nasal mass with striking high signal intensity extending through the posterior choanae into the nasopharynx.

B, Axial T1-weighted image (600/20) shows bilateral, symmetrical nasal masses of homogeneous signal intensity. They are hyperintense relative to muscle but less hyperintense than fat. They extend through the anterior nares and posterior choanae. Hypointense fluid is seen in both maxillary sinuses.

C, Axial T2-weighted image (2500/80) shows the nasal masses are hyperintense relative to fat and muscle but less hyperintense than retained fluid. Small areas of hypointensity are present.

D, Photomicrograph of a resected specimen. Many Mikulicz cells (*arrows*) are present with scattered Russell bodies (*arrowheads*) and many plasma cells (hematoxylin-eosin, original magnification ×400).
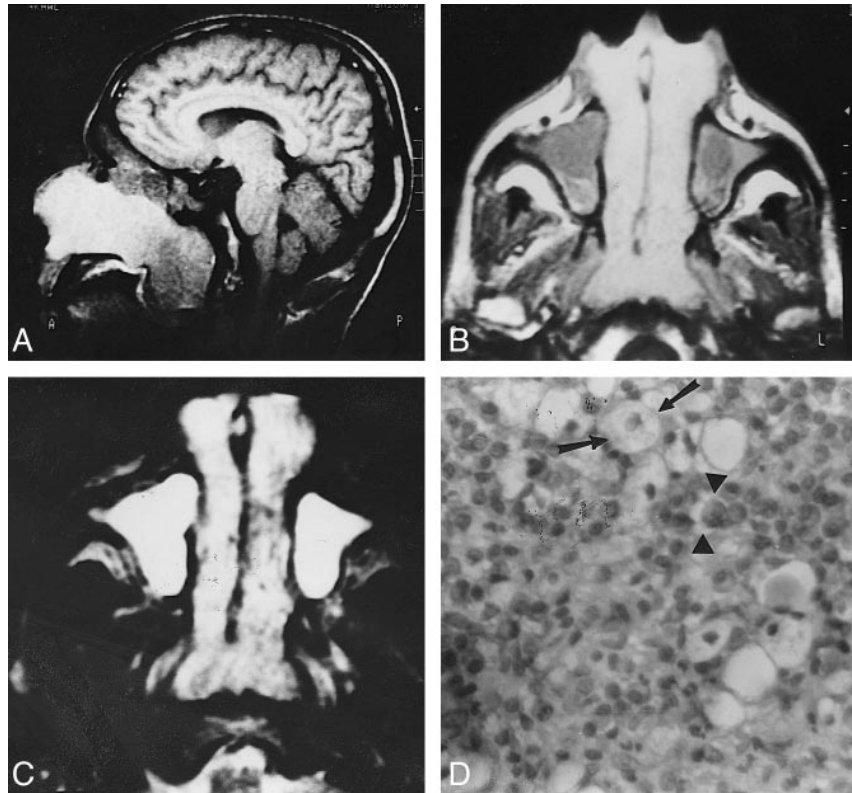
or years, with progressive obstruction of the nasal cavity and signs related to the extension of the mass. 3) The sclerotic (fibrotic) stage is characterized by nasal and/or laryngeal scarring with variable but often severe dyspnea (1, 3, 5).

Methods

A prospective study was conducted in 15 patients with known rhinoscleroma selected from the ENT department. Nine patients were male and six were female; ages ranged from 13 to 36 years (mean age, 25 years). Presentations included nasal mass (n = 6), nasal disfigurement (n = 6), and nasal obstruction (n = 7). The course of the disease was from 2 to 5 years. Rhinoscleroma was diagnosed clinically and proved histopathologically in the hypertrophic stage. Six patients were receiving antibiotic therapy (streptomycin sulfate) at the time of imaging. Biopsies of the nasal masses were done 2 to 6 months before the MR examination.

All MR examinations were performed at our institution on a 1.5-T system using spin-echo pulse sequences. The imaging protocol included axial, coronal, and sagittal T1-weighted images (600–800/20–25/2 [TR/TE/excitations]) and axial and coronal T2-weighted images (2000–2500/30, 80/2). The matrix was 192 × 256, the field of view was 25 cm, and the section thickness was 5 mm. Contrast material was not used.

Images were evaluated for the signal intensity of the nasal masses. For this purpose, all the level settings were made similar on both T1- and T2-weighted sequences. The signal intensity of rhinoscleroma was compared with that of fat, muscle, and CSF on both T1- and T2-weighted images, and was qualitatively classified as striking, moderate, or mildly increased.

Results

Rhinoscleroma appeared as a diffuse, bulky, soft-tissue mass located in the nasal cavities. The nasal masses were bilateral and symmetrical in six patients (Fig 1), bilateral and asymmetrical in four patients (Fig 2), and unilateral in five patients. They were seen in the lower half (n = 6) or along the whole length of the nasal cavity (n = 9) with partial (n = 5) or complete (n = 10) occlusion of the nasal airway. They were associated with thinning of the inferior nasal turbinate (n = 2) and medial wall of the maxillary sinus (n = 1). They extended anteriorly through the anterior nares (n = 9) (Figs 1B and 2B) and posteriorly through the posterior choana into the nasopharynx (n = 3) (Fig 1A–C).

On T1-weighted images, rhinoscleroma showed striking (n = 9) (Fig 1A and B) or mildly (n = 6) (Fig 2A and B) homogeneous high signal intensity. The masses were hyperintense relative to muscle and CSF but less hyperintense than fat. On T2-weighted images, they showed mildly homogeneous hyperintensity (n = 6) or heterogeneous high signal intensity, associated with hypointense foci (n = 9) (Fig 1C). They were hyperintense relative to fat and muscle but less hyperintense than CSF.

Rhinoscleroma obstructed the ostiomeatal unit in 10 patients, with subsequent retained secretions in the maxillary (n = 10) (Fig 1) and ethmoidal (n = 8) sinuses. However, the masses did not actually extend into the paranasal sinuses. On T1-weighted images, rhinoscleroma was hyperintense relative to the retained secretions (Fig 1B) while on T2-weighted images they were less hyperintense than the retained secretions (Fig 1C).
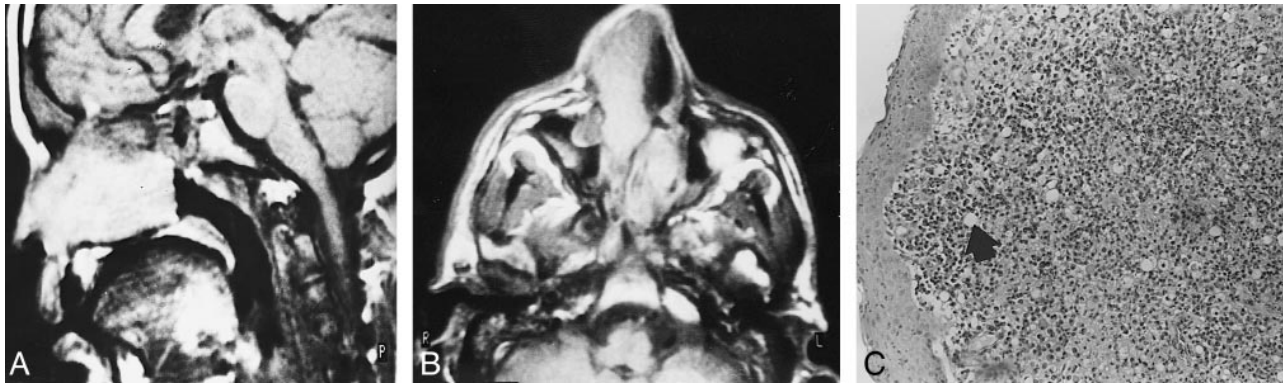
FIG 2. Bilateral asymmetrical rhinoscleroma.
A, Sagittal T1-weighted image (600/25) shows a homogeneously hyperintense nasal mass.
B, Axial T1-weighted image (600/25) shows bilateral asymmetrical nasal masses. The one on the right extends through the anterior nares. They are hyperintense relative to muscle but less hyperintense than fat.
C, Photomicrograph of a resected specimen. Intact squamous epithelium overlies heavy infiltration by chronic inflammatory cells with clear Mikulicz cells (*arrow*) and plasma cells, including Russell bodies (hematoxylin-eosin, original magnification ×100).

Discussion

MR imaging has become the method of choice for the evaluation of many diseases of the head and neck. Rhinoscleroma is a common granulomatous disease in many parts of the world, including the Middle East and South America. The nose is the most common site of infection; however, the nasopharynx, paranasal sinuses, and oropharynx may be involved as well. The disease is not fatal except when stenosing laryngeal or tracheal lesions occur (3). To our knowledge, only a limited number of studies have described the MR imaging features of rhinoscleroma (9), yet knowledge of the MR characteristics of this disease may have an important impact on the method by which it is managed.

Treatment of rhinoscleroma is antibiotic therapy. The most effective antibiotics are streptomycin and tetracycline (10). Local application of 2% acriflavine solution has been reported to produce complete cure of the disease (11). Surgical therapy is usually reserved for excision of obstructing cicatrices. In the event of airway obstruction (eg, laryngeal scarring), tracheostomy may be required (1).

Rhinoscleroma is usually bilateral but it may be of limited extension or of asymmetrical distribution (12, 13). The disease can progress toward the ethmoidal, sphenoidal, frontal, and maxillary sinuses (14, 15), protrude from the anterior nares, or infiltrate the upper lip (13, 15). Superiorly, it can invade the lacrimal sac and orbits (16), and a case of intracranial extension has been described (17). Posteriorly, the mass can protrude from the posterior choanae and affect the eustachian tube and middle ear (13, 14). In our patients, rhinoscleroma masses were bilateral (67%) and unilateral (33%). They may be symmetrical or asymmetrical, and extend into the anterior nares and/or posteriorly through the posterior choanae into the nasopharynx.

The middle and inferior turbinates are always affected, with atrophy or complete destruction, and the nasal septum is frequently destroyed. Involvement of the sinus wall is less common; when present, it consists of displacement or complete absorption of bone related to the chronic progression of this benign disease (5, 14, 16). We found resorption of the inferior turbinate and thinning of the sinus wall.

One of the MR imaging features most relevant to diagnostic analysis is signal intensity. Several recent studies have attempted to differentiate the lesions that occur in the sinonasal cavity by means of their signal intensity on MR images. On T1-weighted studies, both neoplasm and infection have low signal intensity. On T2-weighted sequences, most neoplasms have intermediate signal intensity while an inflamed or obstructed sinus has bright signal intensity. Granulomatous diseases in the sinonasal cavities have low to intermediate signal intensity on all imaging sequences (18–20).

In this series, rhinoscleroma showed mild to marked high signal intensity on both T1- and T2-weighted images. This high signal intensity is attributed to the relatively short T1 and T2 relaxation times of these masses. The high signal on T1-weighted images is quite unusual and striking, and may be a characteristic finding that suggests the diagnosis.

The high signal intensity of rhinoscleroma on T1-weighted images (Fig 1D) may be explained by the high protein content within the Mikulicz cells and Russell bodies. Sometimes, cell breakdown products are hyperintense, perhaps because cholesterol and other fats from the cell membrane are released, but there was no chemical shift artifact. The high signal intensity may have been due to subacute hemorrhage, but there was no other evidence of blood products or of a hypointense rim of hemosiderin. The slightly high signal intensity on T2-weighted images (Figs 1D and 2C) may be attributed to the high cellular component of rhinoscleroma, mainly Russell bodies and Mikulicz cells. Hypointense foci within these lesions may be attributed to areas of fibrosis. Further studies

are recommended to characterize the nature of rhinoscleroma.

To our knowledge, only one description of the MR imaging appearance of rhinoscleroma has been reported (9). Contrary to our findings, this case appeared as a homogeneous mass; isointense on T1-weighted images and of low signal intensity on T2-weighted images. The discrepancy with our findings may be explained by the later stage of the disease, in which there was extensive fibrosis and scarring.

In our study, rhinoscleroma obstructed the ostio-meatal unit, with retained fluids in multiple sinuses. These were clearly differentiated from rhinoscleroma by their signal intensity characteristics. This is in agreement with other studies (17–19), in which MR imaging differentiated tumor from benign processes, such as inflammatory tissue and retained secretions, on the basis of differences in proton mobility.

Conclusion

The hypertrophic stage of rhinoscleroma has characteristic mild to marked high signal intensity on both T1- and T2-weighted MR images.

References

1. Ballenger JJ. **Granulomas of the face, nose, oral cavity and neck.** In: *Diseases of the Nose, Throat, Ear, Head and Neck.* 14th ed. Philadelphia: Lea & Febiger; 1991:314–323
2. Michaels L. *Ear, Nose and Throat Histopathology: Infections.* London: Springer; 1987:137–151
3. Wilson WR, Montgomery WW. **Infectious diseases of the paranasal sinuses.** In: Paparella MM, Shumrick DA, Gluckman JL, Meyerhoff WL, eds. *Otolaryngology, III: Head and Neck.* 3rd ed. Philadelphia: Saunders; 1991:1843–1860
4. Ssali CL. **The management of rhinoscleroma.** *J Laryngol Otol* 1975;89:91–99
5. Becker TS, Shum TK, Waller TS, et al. **Radiological aspects of rhinoscleroma.** *Radiology* 1981;141:433–438
6. Friedmann I. **Electron Microscopy of rare diseases of the nose.** *Trans Am Acad Ophthalmol Otolaryngol* 1963;67:261–280
7. Toppozada H, Riad W, Michaels L, Gaffar H, Sid-Ahmed K. **The epithelium and chronic inflammatory cells in scleroma.** *J Laryngol Otol* 1981;95:1049–1057
8. Gonzalez-Angulo A, Marques-Monter H, Greenberg S, Cerbon J. **Ultrastructure of nasal scleroma.** *Ann Otol Rhinol Laryngol* 1965;74:1022–1033
9. Le Hir P, Marsot-Dupuch K, Bigel P, et al. **Rhinoscleroma with orbital extension: CT and MRI.** *Neuroradiology* 1996;38:175–178
10. Weir N. **Acute and chronic inflammations of the nose.** In: Kerr AG, Groves J, eds. *Scott-Brown's Otolaryngology.* 5th ed. London: Butterworth; 1998:115–141
11. Shaer M, Rizk M, Shawaf E, Ali M, Hashash M. **Local acriflavine: a new therapy for rhinoscleroma.** *J Laryngol Otol* 1981;95:701–706
12. Shehata MA, El-Sallab R, Mandour MA. **Radiographic study of scleroma.** *J Laryngol Otol* 1975;89:1243–1261
13. Yassin A, Badrawy R, Mokhtar M. **Localized forms of rhinoscleroma.** *J Laryngol Otol* 1971;85:269–274
14. Abou Seif SG, Bakry FA, El-Ebrashy F. **Scleroma of the upper air passages: a CT study.** *J Laryngol Otol* 1991;105:198–202
15. Castillo M. **CT findings in a case of pharyngeal rhinoscleroma.** *AJNR Am J Neuroradiol* 1993;14:–770
16. Badrawy R. **Dacryoscleroma (scleroma of the lacrimal passages).** *Ann Otol Rhinol Laryngol* 1962;71:247–251
17. Bahri H, Bassi NK, Rohatgi MS. **Scleroma with intracranial extension.** *Ann Otol Rhinol Laryngol* 1972;81:856–859
18. Som PM, Shapiro MD, Biller HF, Sasaki C, Lawson W. **Sinonasal tumors and inflammatory tissues: differentiation with MR imaging.** *Radiology* 1988;167:803–808
19. Chow JM, Leonetti JP, Mafee MF. **Epithelial tumors of the paranasal sinuses and nasal cavity.** *Radiol Clin North Am* 1993;31:61–73
20. Som PM, Curtin HD. **Sinuses.** In: Stark DD, Bradley WG, eds. *Magnetic Resonance Imaging.* 2nd ed. St Louis: Mosby-Year Book; 1993:1113–1134